THE ANALYSIS OF THE THREE-PHASE INDUCTION MOTOR WITH DEEP ROTOR BARS THROUGH NUMERICAL SIMULATIONS UTILIZING A MODIFIED MATHEMATICAL MODEL

Mihai IORDACHE[1], Sorin DELEANU[2], Neculai GALAN[1]
[1] Politehnica University of Bucharest, Romania
[2]Northern Alberta Institute of Technology, Edmonton, Canada
mihai.iordache@upb.ro, sorind@nait.ca, galannicolae@yahoo.com

Abstract. The three-phase induction machine mathematical model presented in the paper, is adequate for applying to the deep rotor bars case. The rotor resistance $R'_r(\omega_r)$, respectively its leakage inductivity $L'_{r\sigma}(\omega_r)$, depend upon the rotor currents' frequency f_r because of the skin effect. Following the previous considerations, one developed slip dependent analytical expressions of the rotor circuit resistance $R'_r(s)$, respectively rotor circuit leakage reactance $L'_{r\sigma}$ (s). A modified space phasor based mathematical model of the deep bar induction motor is tested through simulations to assess the motor's characteristics. The results are in accordance with the literature.

1.INTRODUCTION

For the induction machine with deep bars in the rotor, the rotor circuit parameters (here referred to the stator), namely the rotor resistance $R'_r(\omega_r)$, respectively its leakage inductivity $L'_{r\sigma}(\omega_r)$ vary with the rotor frequency f_r (or angular frequency ω_r) variation due to the skin effect. Many sophisticated control strategies and mathematical models applied to high-performance drive systems based on the induction motor with deep bars became available in the literature during the last decades [1]-[8]. To calculate the performance characteristics of the three-phase induction motor utilizing its equivalent circuit, one requires the data set values of such a circuit's parameters. Moreover, the rotor parameters are variable due to the presence of skin effect and saturation. The skin effect exercised upon the rotor current is one of the critical factors that affect the simulation's accuracy regarding the three-phase induction motor's mathematical model with deep bars in the rotor. During the years, several methods of study addressed the skin effects present in the rotor bars. For example, one of the models that became classical required the precise representation of the bar's skin effect and its inclusion in the induction motor overall dynamic model. The application across the bar of two voltage signals with different frequencies opens the possibility to follow in real-time the dependency of the bar parameters on frequency, aka frequency characteristic. Such data reach the control system fast enough through a proper transmission [5]. The paper proposes an extended dynamic model, considering the slot neck's saturation and the skin effect, derived from the one from [9]. However, its extensions came in addition to a standard dynamic model

ISSN / ISSN-L: 1843-5912
https://www.doi.org/10.36801/apme.2020.1.15

of the induction machine, their parametrization being relatively easy to achieve. The proposed model adequately addresses the simulations' needs in the time domain, real-time control, and identification processes.

The proposed model, reinforced by comparing it to the finite element analysis and experiments, subjecting one low power induction motor, is legit. The well-known field-oriented control concerning the rotor flux came inadequate for this proposed model of the induction machine because it is impossible to define one unique rotor magnetic flux. Consequently, the rotor "pseudo flux" substituted the original rotor flux in the model, making possible two independent, decoupled controls of the pseudo flux, respectively the torque. The calculation of the induction motor parameters started from the nameplate and its catalog data by applying a straightforward method presented in the paper, with no iterations needed. The method has proven adequate for induction motors presenting deep bars or double cage in the rotor, whereas the rotor parameters' values vary with the slip. When comparing the numerical results obtained with the proposed model for starting torque, breakdown torque, and nominal point of operation to the manufacturer's data, one concludes there is an excellent agreement. Following the proposed methodology's application to hundreds of induction motors, a statistical analysis has proven equivalent circuit parameters determination's relative simplicity without requiring additional data.

This paper presents analytical relationships established for the rotor parameters circuit referred to the stator, as functions of the slip *s*, respectively, for the rotor resistance $R'_r(s)$ and its leakage reactance $L'_{r\sigma}(s)$. Such relationships facilitate the modification of the deep bar induction motor mathematical model from the literature. More precisely, the newly determined analytical relationships complete the existing model, whereas the rotor's voltage equation takes a different form.

2. ELECTRICAL PARAMETERS OF THE INDUCTION MOTOR WITH DEEP BARS

The main reason for the rotor circuit parameters (expressed as referred to the stator) variation with the rotor currents frequency (or angular frequency) is the presence of the skin effect, according to the theoretical data and experimental results. From a thorough analysis of the skin effect subjecting the deep rotor bars of the induction motor, one can conclude that the rotor resistance value referred to the stator $R'_r(\omega_r)$ increases with the increase of the rotor currents' angular frequency ω_r and is approximately proportional to $\sqrt{\omega_r}$. Meanwhile, the leakage inductivity of the rotor $L'_{r\sigma}(\omega_r)$ decreases proportionally to $\sqrt{\omega_r}$. Such assumptions justify the following relationships proposed to express the rotor circuit parameters referred to the stator:

$$R'_r(\omega_r) = R'_r\sqrt{1 + k_R\omega_r}; \quad L'_{r\sigma}(\omega_r) = \frac{L'_{r\sigma}}{\sqrt{1+k_L\omega_r}} \tag{1}$$

Relationships (1) must verify for the ideal no-load data, whereas $\omega_r = 0$, and locked rotor conditions whereas $\omega_r = \omega_s$, ω_s being the angular freequency of the power supply connected to the stator winding.

$$\begin{aligned}\omega_r = 0 \;\Rightarrow\; R_r'(\omega_r) = R_r'(0) = R_r';\quad L_{r\sigma}'(\omega_r) = L_{r\sigma}'(0) = L_{r\sigma}'.\\ \omega_r = \omega_s \;\Rightarrow\; R_r'(\omega_s) = R_{rp}';\quad L_{r\sigma}'(\omega_s) = L_{r\sigma p}'.\end{aligned} \tag{2}$$

With the relationships (1) and (2) as input, one determined the expressions for the factors k_R and k_L, as following:

$$R_r'(\omega_s) = R_{rp}' = R_r'\sqrt{1+k_R\omega_s} \;\Rightarrow\; \left(R_{rp}'\right)^2 = (R_r')^2(1+k_R\omega_s) \;\Rightarrow\; k_R = \left[\left(\frac{R_{rp}'}{R_r'}\right)^2 - 1\right]\frac{1}{\omega_s} = \frac{k_r}{\omega_s}$$

$$L_{r\sigma}'(\omega_s) = \frac{L_{r\sigma}'}{\sqrt{1+k_L\omega_s}} = L_{r\sigma p}' \;\Rightarrow\; \left(L_{r\sigma p}'\right)^2 = \frac{(L_{r\sigma}')^2}{1+k_L\omega_s} \;\Rightarrow\; 1+k_L\omega_s = \left(\frac{L_{r\sigma}'}{L_{r\sigma p}'}\right)^2 \Rightarrow$$

$$k_L = \left[\left(\frac{L_{r\sigma}'}{L_{r\sigma p}'}\right)^2 - 1\right]\frac{1}{\omega_s} = \frac{k_\sigma}{\omega_s} \Rightarrow \tag{3}$$

$$k_R = \left[\left(\frac{R_{rp}'}{R_r'}\right)^2 - 1\right]\frac{1}{\omega_s} = \frac{k_r}{\omega_s};\quad k_L = \left[\left(\frac{L_{r\sigma}'}{L_{r\sigma p}'}\right)^2 - 1\right]\frac{1}{\omega_s} = \frac{k_\sigma}{\omega_s}$$

$$k_r = \left(\frac{R_{rp}'}{R_r'}\right)^2 - 1;\quad k_\sigma = \left(\frac{L_{r\sigma}'}{L_{r\sigma p}'}\right)^2 - 1$$

Substituting (3) in (1), one obtained:

$$\begin{aligned}R_r'(\omega_r) &= R_r'\sqrt{1+k_r\frac{\omega_r}{\omega_s}} = R_r'\sqrt{1+k_r|s|}\\ L_{r\sigma}'(\omega_r) &= \frac{L_{r\sigma}'}{\sqrt{1+k_\sigma\frac{\omega_r}{\omega_s}}} = \frac{L_{r\sigma}'}{\sqrt{1+k_\sigma|s|}};\quad s = \frac{\omega_r}{\omega_s}\end{aligned} \tag{4}$$

where s represents the slip. Many particular solutions to express the induction motor's rotor circuit parameters variation became available in the literature [10] – [16]. However, one can remark the narrowness of a particular solution in regards to solving a specific problem.

3. THE DEVELOPED MATHEMATICAL MODEL

Figure 1 displays the reference frames utilized in the electric machine theory: FS – stator reference frame; FR– rotor reference frame; K– synchronous reference frame. In this paragraph, the induction machine's mathematical model contains the rotor parameters referred to the stator.

The zero-sequence component does not appear due to the floating neutral of the stator winding. The equations, developed using space phasors, appear in the synchronous reference frame, in the following form and with the notations well-known in the literature.

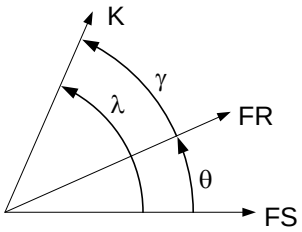

Fig. 1. The axes associated with the reference frame and the angles between them.

$$
\begin{gathered}
u_{sK} = R_{\ s} i_{sK} + \mathrm{j}\omega_K \psi_{sK} + \frac{\mathrm{d}\psi_{sK}}{dt} \\
\psi_{sK} = L_{s\sigma} i_{sK} + L_\mu i_{\mu K} \\
0 = R_r^{'} i_{rK}^{'} + j(\omega_K - \omega)\psi_{rK}^{'} + \frac{\mathrm{d}\psi_{rK}^{'}}{dt} = R_r^{'} i_{rK}^{'} + js\omega_K \psi_{rK}^{'} + \frac{\mathrm{d}\psi_{rK}^{'}}{dt} \\
s = \frac{\omega_K - \omega}{\omega_K} \\
\psi_{rK}^{'} = L_{r\sigma}^{'} i_{rK}^{'} + L_\mu i_{\mu K} \\
u_{sK} = u_{sd} + j u_{sq};\ i_{sK} = i_{sd} + j i_{sq};\ \psi_{sK} = \psi_{sd} + i\psi_{sq} \\
i_{rK}^{'} = i_{rd}^{'} + i i_{rq}^{'};\quad \psi_{rK}^{'} = \psi_{rd}^{'} + j\psi_{rq}^{'} \\
i_{\mu K} = i_{\mu d} + j i_{\mu q} \\
J\frac{\mathrm{d}\Omega}{dt} = M - M_2;\quad M = \frac{3}{2} p\left(\psi_{sd} i_{sq} - \psi_{sq} i_{sd}\right) \\
\frac{d\lambda}{dt} = \omega_K\ = \omega_1;\quad \frac{d\theta}{dt} = \omega \\
R_r^{'}(s) = R_r^{'}\sqrt{1 + k_r|s|} \\
L_{r\sigma}^{'}(s) = \frac{L_{r\sigma}^{'}}{\sqrt{1+k_\sigma|s|}}
\end{gathered}
\tag{5}
$$

One can observe the common term's $L_{\mu}.i_{\mu K}$ presence in the expression of the stator flux ψ_{sK} space phasor and the expression of the rotor flux space phasor $\psi^{'}_{rK}$ referred to the stator. In the equation system (5), no one considered the time variation of the rotor leakage inductivity $L^{'}_{r\sigma}(s)$ referred to the stator. Without neglecting such a variation, the equation (5) determines the form (6):

$$
\begin{gathered}
u_{sK} = R_{\ s} i_{sK} + \mathrm{j}\omega_K \psi_{sK} + \frac{\mathrm{d}\psi_{sK}}{dt} \\
\psi_{sK} = L_{s\sigma} i_{sK} + L_\mu i_{\mu K} \\
\psi_{rK}^{'} = L_{r\sigma}^{'} i_{rK}^{'} + L_\mu i_{\mu K} \\
\frac{\mathrm{d}\psi_{rK}^{'}}{dt} = \frac{d}{dt}\left(L_{r\sigma}^{'} i_{rK}^{'} + L_\mu i_{\mu K}\right) = i_{rK}^{'}\frac{dL_{r\sigma}^{'}}{ds}\frac{\mathrm{d}s}{dt} + L_{r\sigma}^{'}\frac{di_{rK}^{'}}{dt} + L_\mu \frac{di_{\mu K}}{dt}
\end{gathered}
\tag{6}
$$

$$\Rightarrow\ 0 = R_r^{'} i_{rK}^{'} + js\omega_K \psi_{rK}^{'} + \frac{d\psi_{rK}^{'}}{dt} = R_r^{'} i_{rK}^{'} + js\omega_K \psi_{rK}^{'} + i_{rK}^{'} \frac{dL_{r\sigma}^{'}}{ds}\frac{ds}{dt} + L_{r\sigma}^{'} \frac{di_{rK}^{'}}{dt} + L_\mu \frac{di_{\mu K}}{dt}$$

From the equation system (5), one extract the steady state equation of the induction motor, whereas the core loss is negligible (7):

$$\underline{U}_s = R_s \underline{I}_s + j\, X_{s\sigma} \underline{I}_s - \underline{E}_s\ ; \quad 0 = \frac{R_r^{'}}{s} \underline{I}_r^{'} + j\, X_{r\sigma}^{'} \underline{I}_r^{'} - \underline{E}_r^{'}; \tag{7}$$

$$\underline{I}_\mu = \underline{I}_s + \underline{I}_r^{'}; \qquad \underline{E}_r^{'} = \underline{E}_s = -X_\mu \underline{I}_\mu$$

$$M = \frac{3R_r^{'} I_r^{'2}}{s\Omega_1} = \frac{3R_r^{'} U_s^2}{s\Omega_1 \left[\left(R_s + \frac{R_r^{'}}{s}\right)^2 + (X_s + X_{r\sigma}^{'})^2\right]}$$

$$X_{s\sigma} = \omega_1 L_{s\sigma}\ ; \quad X_{r\sigma}^{'} = \omega_1 L_{r\sigma}^{'}\ ; \quad X_\mu = \omega_1 L_\mu$$

4. SIMULATIONS

4.1 Calculated parameters

Table 1 contains the technical specifications of the induction motor used in simulations, with nameplate data including $f_1 =$ 60 Hz ; $2p = 6$; $U_s = U_{fn} = 323.32$V; $I_{fn} = 130$ A. Table 2 displays the parameters of its complete (Steinmetz) equivalent circuit developed for steady-state conditions.

Table 1. Technical specifications of the induction motor

P_n kW	U_n V	I_n A	n_1 rot/min	n rot/min	η_n %	$\cos\varphi_{1n}$ -	i_p -	m_p -	m_m -	J kgm^2	Conex.
100	560	130	1200	1168,8	0,897	0,87	4	1,1	1,8	3,38	wye

Table 2. Equivalent scheme parameters of the induction motor

Z_n [Ω]	R_s [Ω]	$L_{s\sigma}$ [H]	R'_r [Ω]	$L'_{r\sigma}$ [H]	L_μ [H]
2,48	0,053	$1,034 \cdot 10^{-3}$	0,0657	$0,955 \cdot 10^{-3}$	$28,1 \cdot 10^{-3}$

With the data from tables 1 and 2, one calculated the following values:

M_n = 817 Nm (nominal torque), M_p = 898.7 Nm (starting torque), I_p = 520 A (starting current), S_n = 128094.8 VA (input apparent power at nominal conditions of operation), s_n =0.026 (nominal slip), $P_{1n} = S_n \cos\varphi_{1n}$ = 111442.5 W (input real power at nominal conditions of operation), $I_{s0} \cong U_{fn}/X_\mu = 30.53$ A (ideal no-load current in amps), $i_{s0} = I_{s0} / I_{fn} = 0.235 = 23.5$ % (ideal no-load current expressed in per-unit, respectively percent of the nominal current).

The reactances have the following values for a frequency of the power supply equal to 60Hz: $X_{s\sigma}$ = 0.39Ω (stator leakage reactance), $X'_{r\sigma}$ = 0.36Ω (rotor leakage reactance referred to the stator); X_μ = 10.59Ω (magnetizing reactance).

The induction motor parameters from the Steinmetz equivalent circuit of the induction motor, expressed in per-unit have the following values, where $Z_n = U_{fn}/I_{fn}$ is the

base impedance: $r_s = 0.0214$, $r'_r = 0.0262$, $x_{s\sigma} = X_{s\sigma} / Z_n = 0.157$, $x'_{r\sigma} = X'_{r\sigma} / Z_n = 0.145$, $x_\mu = X_\mu / Z_n = 4.27$.

The cyclical inductivities from the expressions of the magnetic fluxes have the following values: $L_s = L_{s\sigma} + L_\mu$ =29.134mH, $L'_r = L'_{r\sigma} + L_\mu$ =29.055mH, L_μ = 28.1mH. From the value of per-unit rotor resistance referred to the stator, one concludes the correctness regarding calculating the nominal slip from technical specification data, which means $r'_r \cong s_n$, i.e., r'_r = 0,0262 ≅ s_n =0,026.

4.2 Dependency of the rotor's electrical parameters on the slip

Expressing the $\sqrt{s}$ dependent rotor parameters referred to the stator in per-unit facilitates comparing the results from the literature.

$$r'_r(s) = \frac{R'_r(s)}{R'_r} = \sqrt{1 + k_r|s|} \qquad (8)$$
$$x'_{r\sigma}(s) = \frac{L'_{r\sigma}(s)}{L'_{r\sigma}} = \frac{X'_{r\sigma}(s)}{X'_{r\sigma}} = \frac{1}{\sqrt{1+k_\sigma|s|}}; \quad s = \frac{\omega_r}{\omega_s}$$

$$r'_r(\sqrt{s}) = f_r(\sqrt{s}) = \sqrt{1 + k_r\sqrt{s^2}}$$
$$x'_{r\sigma}(\sqrt{s}) = f_x(\sqrt{s}) = \frac{1}{\sqrt{1 + k_\sigma\sqrt{s^2}}}; \quad s = \frac{\omega_r}{\omega_s} \qquad (9)$$
$$s \in [0\ ;\ 1{,}2]; \quad k_r = 4,\ 6.5,\ 9;\ k_\sigma = 0.10,\ 0.16, 0.25$$

The values of the factors k_r and k_σ are with an extensive range, corresponding to a trapezoidal-shaped rotor slot. Figure 2 displays the $\sqrt{s}$ (here, namely sqrt(s) in per-unit [%%]) dependent values of the per-unit rotor resistance, respectively per-unit leakage reactance referred to the stator for the values of the k_r and k_σ factors from (9).

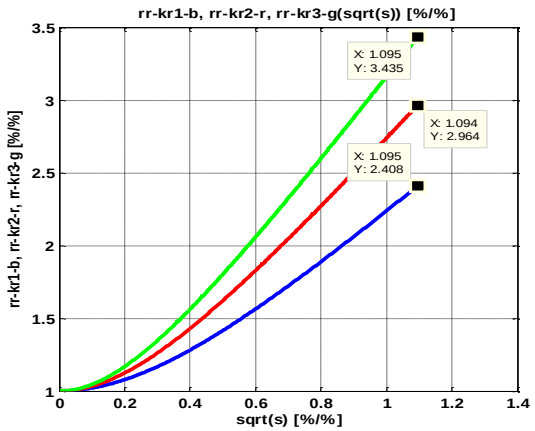

(a)

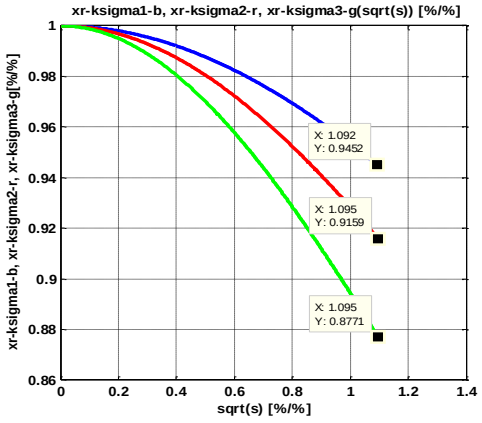

(b)

Fig. 2. a) The per-unit rotor $r_r = f(\sqrt{s})$, for $k_{r1} = 4$, $k_{r2} = 6{,}5$ și $k_{r3} = 9$; b) The per-unit rotor leakage reactance $x'_{r\sigma} = f(\sqrt{s})$, $k_{r\sigma 1} = 0{,}1$, $k_{r\sigma 2} = 0{,}16$ și $k_{r\sigma 3} = 0{,}25$.

Analyzing the curves from figure 2, one remarks the almost linear increase of the rotor resistance referred to the stator $r'_r = f(\sqrt{s})$ with the variable's $\sqrt{s}$ increase. In contrast, the curves representing the rotor leakage reactance referred to the stator $x'_{r\sigma} = f(\sqrt{s})$ display a substantial decay concerning the same variable increasing. Such elements show consistency when compared with the data from literature [17] – [25]. Both families of variation curves from figure 2 are continuous functions, and their derivatives are continuous as well, which has proven useful when one requires differential and integral calculations.

4.3 Steady state developed torque

The expression (10) representing the electromagnetic torque's dependency on the slip contains slip-dependent electric parameters.

$$M = \frac{3R'_r(s)\,U_s^2}{\Omega_1 s\left[\left(R_s + c_1\frac{R'_r(s)}{s}\right)^2 + \left(X_{s\sigma} + c_1 X'_{r\sigma}(s)\right)^2\right]} = \frac{3R'_r U_s^2}{\Omega_1}\,\frac{\sqrt{1 + k_r|s|}}{s\left[\left(R_s + c_1\frac{R'_r(s)}{s}\right)^2 + \left(X_{s\sigma} + c_1 X'_{r\sigma}(s)\right)^2\right]} \tag{10}$$

From (10), one can assess the torque variation as a sequence of steady states, such as being applicable to slow transients. Relationship (10) in conjunction with the rotor parameters' explicit dependency on the slip generates the torque - slip family $M = f_m(\underline{s})$ of curves. Figure 3 contains such a family representation for the data set described by (11).

$$M = f_m(s)\ ;\ s \in [0\ ;\ 1{,}2]$$

$$1)\quad k_r = 4\ ;\quad k_\sigma = 0.10;\quad 2)\quad k_r = 9\ ;\quad k_\sigma = 0.25 \tag{11}$$

$$R_s = 0.053\Omega;\ R'_r = 0.0657\Omega;\ X_{s\sigma} = 0.39\,\Omega;\ X'_{r\sigma} = 0.36\,\Omega;\ X'_\mu = 10.59\,\Omega$$

$$\underline{c_1} = 1 + \frac{\underline{Z_{s\sigma}}}{\underline{Z_0}} \Rightarrow c_1 \approx 1 + \frac{0{,}39}{10{,}59} = 1.037$$

From the curves representing the torque – slip dependency presented in figure 3, one can highlight the significant influence exercised by the factors k_r and k_σ determined by the rotor slot geometry. However, because the breakdown torque values are close, the two factors' influence is almost inexistent. Such a conclusion reflects that the high-power

induction motors develop their breakdown torque for very low values of the slip, whereas the skin effect is practically negligible.

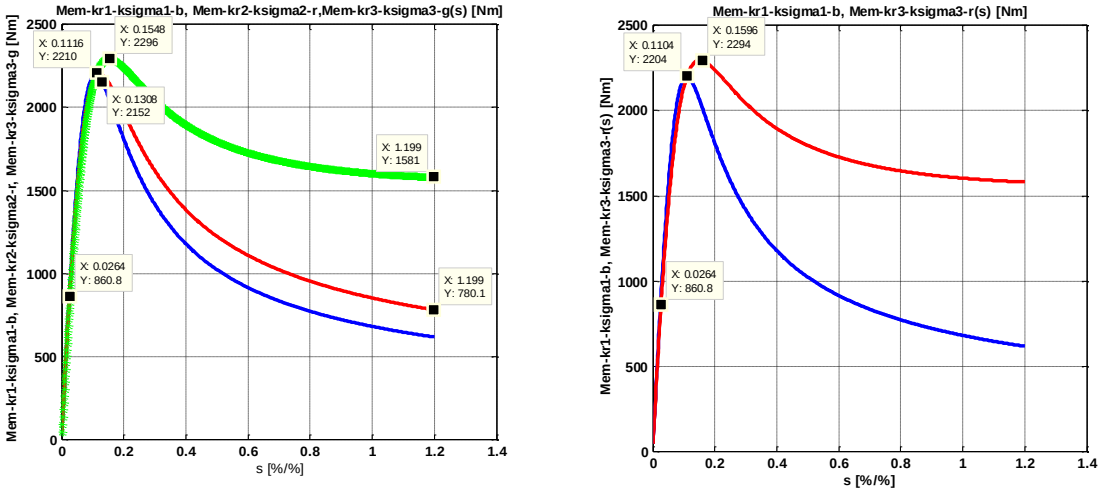

Fig. 3. The dependency of electromagnetic torque on the slip, *M=f(s):* a) for $k_{r1} = 4$ and $k_{\sigma 1} = 0.1$, $k_{r2} = 6.5$ and $k_{\sigma 2} = 0.16$, $k_{r3} = 9$ and $k_{\sigma 3} = 0.25$; b) $k_{r1} = 4$ and $k_{\sigma 1} = 0.1$, $k_{r3} = 9$ and $k_{\sigma 3} = 0.25$.

The values obtained for the staring torque show a substantial increase with the increase of the factor kr, since, at the starting condition, slip is equal to 1, which means the maximum frequency of the rotor currents. In such conditions, the strong skin effect determines the significant increase of the rotor bar resistance, and consequently, a significant increase in factor k_r. There is a large variety of rotor slot geometry (i.e., a large variety of the rotor bar cross-section) experiencing a significant skin effect, resulting in large values recorded by the staring torque.

4.4 Mechanical equation

The motor characteristics' time dependency requires solving the mechanical equation subjecting the induction motor and the load. In this case, the load torque presents two components: constant M_0 and another one sinusoidal versus time with a magnitude M_1. The electromagnetic torque from (12) depends on the induction motor's electric parameters, which are slip dependent themselves.

$$J\frac{d\Omega}{dt} = M - M_2$$

$$\frac{3R_r'U_s^2}{\Omega_1}\frac{\sqrt{1+k_r|s|}}{s\left(R_s + c_1\frac{R_r'\sqrt{1+k_r|s|}}{s}\right)^2 + \left(X_{s\sigma} + c_1\frac{X_{r\sigma}'}{\sqrt{1+k_\sigma|s|}}\right)^2} - (M_0 + M_1\sin\omega t); \quad (12)$$

$$M_0 = 500Nm; M_1 = 100Nm$$

Solving the equation (12), one can develop several sets of curves, for example, the time dependency of the slip, displayed in figure 4. In this case, the starting process has a very short duration (0.2 s) due to the very significant presence of the skin effect, which leads

to a large starting current compared to the one necessary to drive the load at nominal conditions.

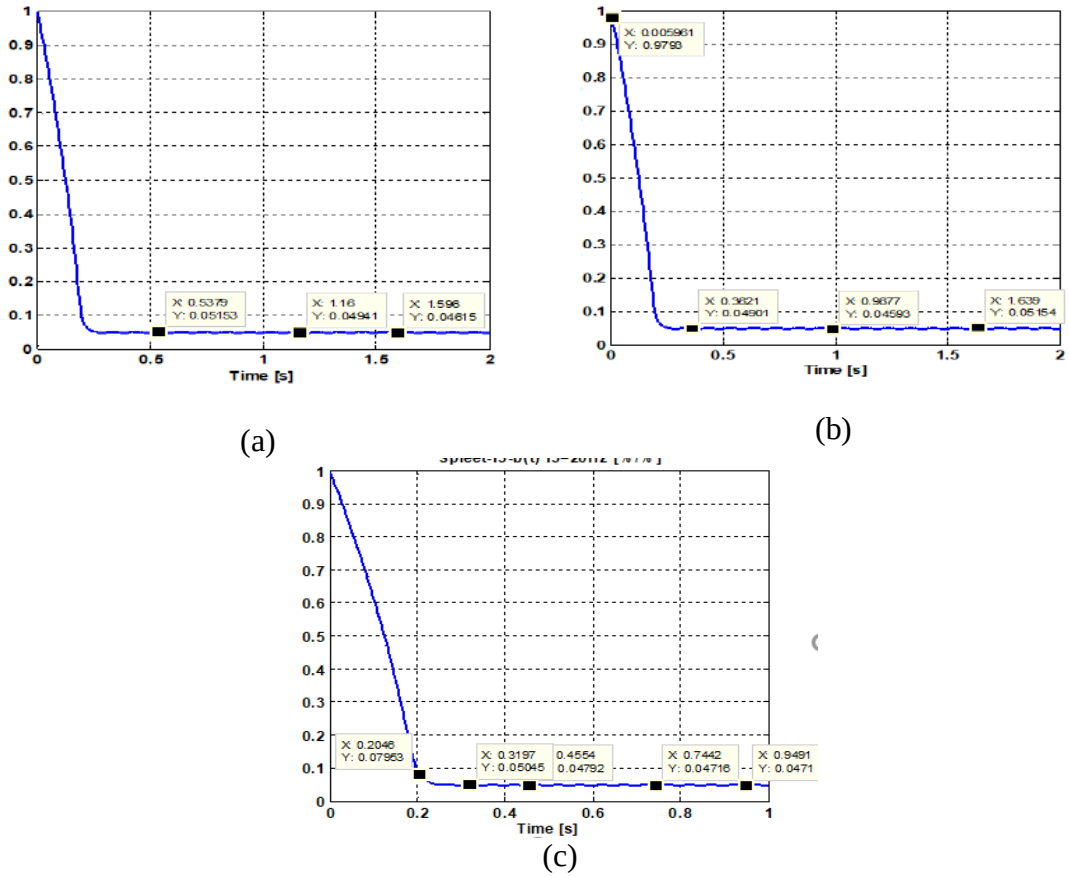

Fig. 4. Time variation of the slip at different frequency values k_r= 9.0, k_σ=0.25: a) f= 0,5 Hz; b) f=10 Hz; c) f=20 Hz.

The load torque component with a sinusoidal variation with time has an average value equal to zero and does not influence the motor starting process. In the steady-state regime, the slip has a small ripple despite the large magnitude of the load torque's sinusoidal component. Such a phenomenon is like the one encountered by the synchronous motor equipped with damper winding, whereas being started in asynchronous conditions across the line.

4.5 Electromagnetic torque developed by the motor during operation

The electromagnetic torque developed by the induction motor has common elements with the no-load torque, as one can figure out, whereas consulting figure 5. All the distortions from the electromagnetic torque appear because of the load torque's presence. However, the curve from figure 5 represents the upper envelope of the original, time oscillating developed electromagnetic torque, available in MATLAB through instruction as [up, lo] =envelope(torque,50,'peak').During the starting process, the resultant torque accelerates the rotor, whereas, during the steady-state, the electromagnetic torque developed by the induction motor equals the load torque, the rotation being assured by the average torque.

Figure 6 displays the mechanical characteristic $n_r = f(M_{em})$ for $k_{r3} = 9$, $k_{\sigma 3} = 0.25$ and $f = 0.5$ Hz.

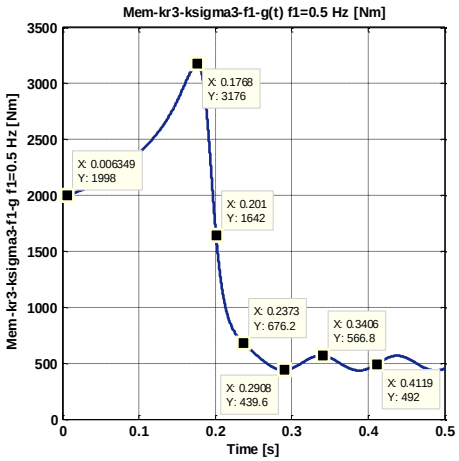

Fig.5. Time variation of the electromagnetic torque for $k_{r3} = 9$, $k_{\sigma 3} = 0.25$ and $f = 0.5$ Hz.

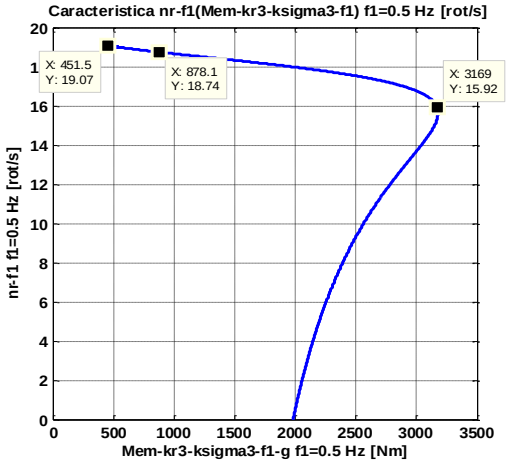

Fig.6. Mechanical characteristic $n_r = f(M_{em})$ for $k_{r3} = 9$, $k_{\sigma 3} = 0.25$ and $f = 0.5$ Hz.

5. CONCLUSION

This paper contains the analysis of the rotor electrical parameters' variation with the rotor current frequency due to the skin effect. More precisely, the analysis targeted the resistance $R'_r(\omega_r)$, respectively leakage inductivity $L'_{r\sigma}(\omega_r)$, of the rotor with deep bars, whereas both rotor parameters are referred to the stator. The analytical expressions representing the slip dependency of the rotor parameters derived in this paper are valid for each operating regime. The well-known mathematical model suffered adaptations, the additions transforming it into a model suitable to represent the induction motor with deep bars in the rotor. For the slow transient regimes, the completion of the equation system requires the addition of the expressions regarding the rotor resistance, respectively rotor leakage reactance, both refereed to the stator, depending on the slip, without modifying the voltage equations. To apply the equation system at the full extent of every single operation regime, one demands the modification of the rotor's voltage equation: in the electric circuit of the rotor, one senses the presence of an electromotive force due to the time variation of the rotor's leakage inductance. The results obtained through simulations applied to the new mathematical model demonstrate a full consistency with the literature's data. The obtained characteristics represent continuous functions, their first derivatives being continuous, which has a positive impact regarding further calculations involving derivation and integration. The physical basis of the introduced model may be useful for cases of analysis.

REFERENCES

[1] P. Vas, Parameter Estimation, Condition Monitoring, and Diagnosis of Electrical Machines. London, U.K.: Clarendon, 1993.

[2] J. K. Seok and S. K. Sul, “Induction motor parameter tuning for high-performance drives,” IEEE Trans. Ind. Appl., vol. 37, no. 1, pp. 35–41, Jan./Feb. 2001.
[3] J. K. Seok, D. W. Chung, S. H. Song, S. K. Sul, B. K. Kwon, G. W. Park, W. C. Shin, E. S. Cho, J. S. Lee, and C. H. Choi, “A new approach to advanced cold mill drive systems,” in Conf. Rec. IEEE IAS Annual Meeting, pp. 2125–2130, 1997.
[4] M. A. Valenzuela, J. M. Bentley, and R. D. Lorenz, “Sensorless tension control in paper machines,” IEEE Trans. Ind. Appl., vol. 39, no. 2, p. 294–304, 2003.
[5] J. R. Willis, G. J. Brock, and J. S. Edmonds, “Derivation of induction motor models from standstill frequency response tests,” IEEE Trans. Energy Convers., vol. 4, no. 4, pp. 608–613, 1989.
[6] S.I. Moon and A. Keyhani, “Estimation of induction machine parameters from standstill time-domain data,” IEEE Trans. Ind. Appl., vol. 30, no. 6,pp. 1609–1615, 1994.
[7] R. W. A. A. De Doncker, “Field-oriented controller with rotor deep bar compensation circuits,” IEEE Trans. Ind. App., vol. 28, pp.1062–1071, 1992.
[8]. Jul-Ki Seok, Seung-Ki Sul, “Pseudorotor-Flux-Oriented Control of an Induction Machine for Deep-Bar-Effect Compensation,” IEEE Trans. on Ind. Appl. , vol: 34 , no.3 , p**:** 429 – 434, 1998.
[9]. R. C. Healey, S. Williamson, and A. C. Smith, “Improved cage rotor models for vector-controlled induction motors,” IEEE Trans. Ind. Appl., vol. 31, pp. 812–822, 1995.
[10]. J.M Correea-Guimaraes, J.V. Bernardes, E. Hermeto, and E. da Silva, “Parameter Determination of Asynchronous Machines from Manufacturer Data Sheet,” IEEE Trans. Ener. Conv., vol. 29, no. 3, pp. 689 – 697, 2014.
[11] P. C. Krause, O. Wasynczuk, and S. D. Sudhoff, Analysis of Electric Machinery. New York, NY, USA: IEEE Press, 1995.
[12] M. Kostenko and L. Piotrovsky, Electrical Machines—Part 2. Moscow, USSR: Mir Pub., 1977.
[13] Test Procedure for Polyphase Induction Motors and Generators. IEEE Standard 112, 2004.
[14] Rotating Electrical Machines. Part 2-1: Standard Methods for Determining Losses and Efficiency From Tests, IEC Standard 60034-2-1, 2007.
[15] M. S. Zaky, M. M. Khater, S. S. Shokralla, and H. A. Yasin, “Wide-speed-range estimation with online parameter identification schemes of sensor-less induction motor drives,” IEEE Trans. IE, vol. 56, no. 5, pp. 1699–1707, 2009.
[16] M. Wlas, Z. Krzemin ski, and H. A. Toliyat, “Neural-network-based parameter estimations of induction motors,” IEEE Trans. IE, vol. 55, no. 4, pp. 1783–1794, 2008.
[17] GHEORGHIU I.S., FRANSUA A., *Tratat de maşini electrice*, Vol.I – Maşina de curent continuu, 1968. Vol. II – Transformatoare, 1970. Vol. III – Maşini asincrone, 1971. Vol. IV – Maşini sincrone, 1972. Editura Academiei R.S.R. Bucureşti. (In Romanian)
[18] DORDEA, T. Maşini electrice, vol. I (2002) – Teorie, vol. II (2003) – Proiectare, vol. III (2003)– Construcţie, Editura ASAB, 2002 – 2003, Bucureşti. (In Romanian)
[19] BOLDEA, I. Parametrii maşinilor electrice, Editura Academiei Române, Bucureşti, 1991. (In Romanian)
[20] CÂMPEANU, A. Maşini electrice. Probleme fundamentale, speciale şi de funcţionare optimală. Editura Scrisul Românesc, Craiova, 1988. (In Romanian)
[21] MIHALACHE, M. Maşini electrice, volumul 1 –Transformatoare electrice, 1994; volumul 2 – Maşini electrice rotative, 1996, Universitatea Politehnica din Bucureşti. (In Romanian)
[22]. GALAN, N. Masini electrice, Editura Academiei Romane, Bucuresti, 2011. (In Romanian)
[23]. C. Grantham and D. J. McKinnon, “Rapid parameter determination for induction motor analysis and control,” IEEE Trans. Ind. Appl., vol. 39, no. 4, pp. 1014–1020, Jul./Aug. 2003.
[24] P. Pillay, R. Nolan, and T. Haque, “Application of genetic algorithms to rotor parameter determination from transient torque calculations,” IEEE Trans. Ind. Appl., vol. 33, no. 5, pp. 1273–1282, Sep./Oct. 1997.
[25] V. P. Sakthivel, R. Bhuvaneswari, and S. Subramanian, “Multi-objective parameter estimation of induction motor using particle swarm optimization,” Eng. Appl. Art. Int., vol. 23, pp. 302–312, 2010.